

## Diffusion-layer microstructure of Ni on Si(100)

Yu-Jeng Chang and J. L. Erskine

*Department of Physics, The University of Texas at Austin, Austin, Texas 78712*

(Received 24 May 1982)

The initial stage of nickel silicide compound formation at Si(100) surfaces is investigated using low-energy electron diffraction and ultraviolet photoemission spectroscopy. Experimental evidence is obtained for the postulated high interface mobility resulting from transforming the bonding of interface Si atoms from covalent to metallic character. The bond transformation is induced by nickel atoms occupying tetrahedral interstitial voids of the Si lattice. The observed interstitial Ni *d*-state binding energy suggests a diffusion-layer microstructure which does not favor nickel-atom occupancy of adjacent tetrahedral voids.

Structural and stoichiometric variation of the interfacial region are key parameters which relate metal semiconductor interface microstructure and Schottky barriers heights.<sup>1-4</sup> Recent experimental studies of metal semiconductor interfaces<sup>5-8</sup> have begun to provide a picture of the structure, stoichiometry, interface width, and growth kinetics of this important class of compounds. One of the more interesting results of these studies is the observation of selective growth of silicides,<sup>9</sup> and the related fact that metal rich silicides form at temperatures far below the melting point of Si. For example, Si melts at 1383 °C, whereas the formation temperature for Ni<sub>2</sub>Si is only 200 °C.

One explanation for the tendency of metal rich silicides to form at such low temperatures is based on an interstitial defect model.<sup>9</sup> The energy required to break a Si covalent bond at a low-index surface is of the order of 3 eV. Therefore, it is energetically unfavorable for Si atoms to initiate compound formation at 200 °C, and kinetically impossible to generate the Si flux across the interface needed to sustain growth without a substantial reduction in the Si covalent bond strength. The interstitial defect model overcomes this problem. Ni atoms deposited onto Si surfaces are assumed able to occupy interstitial voids in the Si lattice with very little activation energy. Charge transfer between adjacent Ni and Si atoms occurs, and the local Si covalent bonds transform to weaker metalliclike bonds. This interstitial atom induced bond transformation produces the reduced Si bond strength needed to account for low-temperature silicide compound formation.

Recent experimental work on thin film metal silicon compounds has provided some support for the interstitial void model of silicide formation and has yielded important insight into the reactivity and interface structure of silicide compounds. Ion channeling techniques have been used to investigate interfacial order and reactivity of epitaxial nickel silicides<sup>5</sup> as well as lattice site location of low coverages of Ni on

Si crystals.<sup>6</sup> The latter study shows that low-level coverages of Ni deposited on Si(100) at room temperature produce a dispersed Ni-Si interface with  $\sim 2 \times 10^{15}$  Ni atoms/cm<sup>2</sup> occupying tetrahedral interstitial voids of the Si lattice. X-ray photoelectron spectroscopy<sup>7</sup> has also been used to study the chemical nature of the Ni-Si interface. This study shows that Ni-Si interfaces, produced by room-temperature deposition of Ni onto Si, are characterized by a region of graded composition. Both of these results provide indirect evidence for compound formation based on the interstitial defect model.

In this paper we present additional evidence of the formation of metallic interstitials in Si lattice voids. Our results also suggest a specific model for the diffusion layer microstructure of low coverage Ni layers on Si surfaces. In this model Ni atoms occupy tetrahedral voids in the Si lattice, but tend not to occupy adjacent sites.

Our experiments were carried out by using a spectrometer, described previously,<sup>10</sup> which combines several probes including low-energy electron diffraction (LEED), high sensitivity Auger spectroscopy, and angle resolved photoemission. A vacuum evaporation source and quartz-crystal microbalance provided additional capability needed to prepare and accurately monitor thin metal overlayers *in situ*. Samples could be heated radiatively to over 1000 °C and cooled to 40 K. Typical base pressures were  $1 \times 10^{-10}$  Torr ( $3 \times 10^{-10}$  Torr He during resonance lamp operation and  $9 \times 10^{-9}$  Torr during Ni deposition).

The  $\frac{3}{8}$ -in.-diameter  $\times$  0.020-in.-thick Si targets were cut from B-doped 50- $\Omega$  cm oriented (100) wafers provided by Monsanto. The targets were clamped to a ceramic ring by two 0.030-in.-diam W wires. This minimized compound formation from mounting-assembly electrodes. The sample temperature was measured by a W-5 at. % Re vs W-26 at. % Re thermocouple in mechanical contact with the sample. Targets were degreased by standard techniques and cleaned *in situ* by repeated argon-ion sputtering

(500 eV,  $10 \mu\text{A}/\text{cm}^2$ ) and annealing ( $800^\circ\text{C}$ ). This procedure produced surfaces which yielded sharp  $(2\times 1)$  LEED patterns, distinct surface state peaks in photoemission spectra, and no indication from Auger analysis of contamination. Nickel was deposited on the clean Si surfaces at rates of  $\sim 1 \text{ \AA}/\text{min}$  by evaporation from 99.99%-pure Ni wire wrapped on a W filament.

Figure 1 shows photoelectron spectra ( $\hbar\omega=21.22 \text{ eV}$ ) for clean Si(100) and for Si(100) after several sequences of deposition and annealing. The lower two spectra are angle-integrated spectra for clean Si(100) before and after deposition of  $0.25 \text{ \AA}$  of Ni ( $2.3\times 10^{14}/\text{cm}^2$ ). The sample was maintained at room temperature during and after evaporation for the angle integrated spectra. All clean Si(100)- $(2\times 1)$  surfaces exhibited photoemission spectra surface state peaks<sup>11,12</sup> at  $-0.80$  and  $-1.17 \text{ eV}$  binding energy measured from the Fermi level  $E_F$ . ( $E_F$  was accurately determined after completing the low coverage studies by forming a metallic silicide on the target.) Evaporated Ni layers  $0.25 \text{ \AA}$  thick which are not annealed disrupt the surface state peaks (as shown by Fig. 1) and reduce the sharpness of the  $(2\times 1)$  LEED

pattern. Surface state peaks and the  $(2\times 1)$  LEED pattern are destroyed at Ni coverages of  $\sim 1.5 \text{ \AA}$ .

The upper curves in Fig. 1 are angle resolved photoelectron spectra for clean Si(100)  $(2\times 1)$  before and after sequential deposition of Ni followed by annealing. The surface states observed in photoelectron spectra for clean Si(100) and the  $(2\times 1)$  LEED pattern disappeared after each Ni deposition step, but both reappear after a brief annealing cycle (60 sec). The diffusion layer microstructure appears to be temperature independent for annealing between  $200$ - $800^\circ\text{C}$ . Also, prolonged annealing (below  $800^\circ\text{C}$ ) does not tend to deplete the concentration of Ni atoms in the diffusion layer. Hansson *et al.*<sup>8</sup> report observing the same effect. Apparently Ni atoms are bound most tightly in interstitial voids near the surface. Auger analysis after each annealing step indicated that Ni atoms diffuse into and remain near the surface (within the escape depth of Ni Auger electrons). Also, the difference between photoemission spectra of clean Si surfaces and surfaces with diffused Ni atoms yields the  $d$ -state binding energy of Ni atoms in the Si lattice host. Reemergence of the two surface states and Si bulk states in the photoelectron spectra, and reestablishment of the  $(2\times 1)$  LEED pattern is strong evidence that the diffused Ni atoms occupy sites which cause minimal perturbation of the Si host lattice. The tetrahedral interstitial voids are the most likely locations. It is also clear that  $\text{NiSi}_2$  is not formed initially at the low coverages reported here. We have studied the electronic structure of epitaxial  $\text{NiSi}_2$  on Si(111) and on Si(100) surfaces.<sup>13</sup> These ordered compounds produce  $(1\times 1)$  LEED patterns and epitaxially grown  $\text{NiSi}_2$  on Si(100) does not exhibit any photoelectron peaks similar to the two surface state peaks shown in Fig. 1.

The photoelectron spectra in Fig. 1 exhibit evidence for Si bond transformation due to the Ni interstitials and also contain information pertaining to the diffusion layer microstructure of the Ni atoms in the Si lattice host. When Ni has diffused into interstitial sites of the Si lattice, the surface state binding energies are observed to decrease to  $-0.70$  and  $-0.99 \text{ eV}$ . This shift is consistent with calculated ionicities<sup>14</sup> of silicide compounds (for example, in  $\text{NiSi}_2$  these are: Ni,  $+1.119$  electrons; Si,  $-0.560$  electrons) and indicates that the Si bonds are indeed weakened by the presence of the Ni interstitials. Although the absolute binding energy shifts are small, the relative change in relation to the clean surface state binding energy is nearly 30%. Shaded regions between spectra for clean Si surfaces and the surfaces with diffused Ni atoms indicate  $d$ -state photoemission resulting from interstitial Ni atoms. The binding energy is approximately  $2.78 \text{ eV}$  measured from  $E_F$ .

The  $d$ -state binding energy for interstitial Ni atoms in Si is characteristic of their local environment. Figure 2 illustrates photoelectron spectra for  $\text{Ni}_2\text{Si}$ ,  $\text{NiSi}$ ,

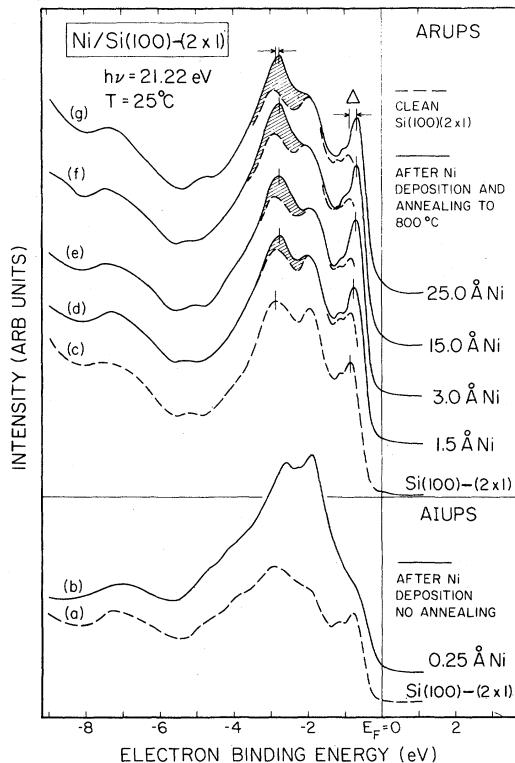


FIG. 1. Photoemission spectra for Si(100) surfaces before and after sequential deposition of Ni and annealing. Lower two curves, angle integrated spectra for clean Si(100)- $(2\times 1)$  before and after room-temperature deposition of  $0.25 \text{ \AA}$  of Ni. Upper curves, angle-resolved spectra for sequential deposition of Ni followed by annealing.

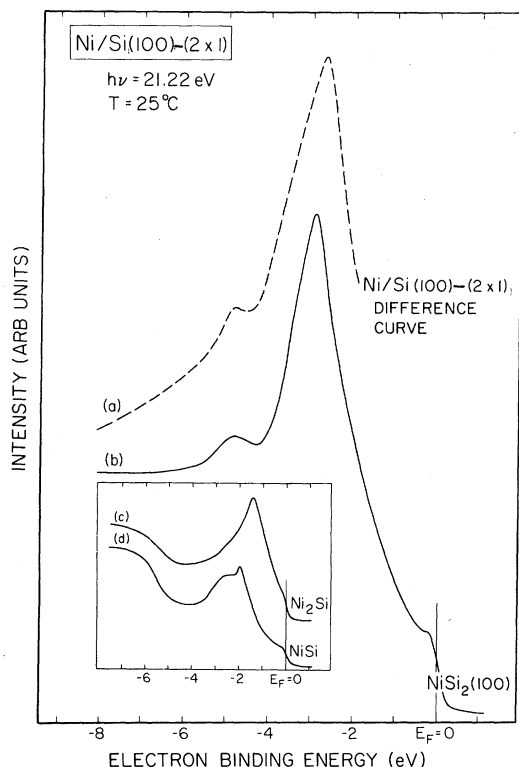


FIG. 2. Solid curves angle-resolved photoemission spectra for  $\text{Ni}_2\text{Si}$ ,  $\text{NiSi}$ , and  $\text{NiSi}_2$  compounds produced by annealing thick deposited Ni films on  $\text{Ni}(100)$ ; dashed curve difference spectra obtained by subtracting  $\text{Si}(100)-(2 \times 1)$  spectra from spectra for  $1.5 \text{ \AA}$  Ni deposited on  $\text{Si}(100)$  and annealed (see text).

and  $\text{NiSi}_2$  films produced by vacuum evaporating Ni on  $\text{Si}(100)$  and annealing at the appropriate temperatures.<sup>15</sup> The spectra are dominated by emission from Ni  $d$  states. A clear trend is apparent in the  $d$ -level peak widths and position for the three stoichiometries represented by these compounds: The Ni-rich silicide compound  $\text{Ni}_2\text{Si}$  exhibits broader  $d$ -state peaks at

lower binding energies than does the Si-rich compound  $\text{NiSi}_2$ ; parameters for  $\text{NiSi}$  fall between those of the other two compounds. The spectra corresponding to the diffusion layer are identical to those of  $\text{NiSi}_2$ . This trend has also been observed in angle-integrated photoemission studies covering a broad photon energy range by using synchrotron radiation and cleaved bulk crystals.<sup>16</sup> These results and closely related theoretical work<sup>14,17</sup> imply that the  $d$  states do not play a dominant role in the Ni-Si bonds but do tend to reflect the Ni-Ni neighbor distance and coordination number through the  $d$ -state interactions.

To better understand how the results of Fig. 2 relate to the diffusion layer microstructure, we summarize in Table I selected parameters for three models of the diffusion layer. Recent thin-crystal channeling experiments<sup>6</sup> have yielded a model for low coverages of Ni atoms deposited at room temperature onto  $\text{Si}(100)$ . The channeling results are explained by a diffusion layer microstructure model (model No. 1) which assumes Ni atoms occupy all available Si lattice interstitial voids near the surface. The channeling data are incompatible with any of the crystal structures of nickel silicides ( $\text{Ni}_2\text{Si}$ ,  $\text{NiSi}$ , and  $\text{NiSi}_2$ ) and the initial formation of one of these phases can be ruled out. Our results for diffused Ni  $d$ -state binding energy suggest that the Ni atom environment is more closely approximated by a model (model No. 2 in Table I) which assumes that only every other interstitial site is occupied by Ni atoms. Another way of stating model No. 2 is that in this model, Ni atoms in the diffusion layer have an fcc structure rather than the diamond structure. Table I shows that in model No. 2, Ni atoms have the same structure and stoichiometry as they do in  $\text{NiSi}_2$ , and the Ni-Ni neighbor coordination and distances are nearly identical. This accounts for the very similar local environment and thus the similar  $d$ -state binding energies.

Figure 3 illustrates our new model for low coverage diffused Ni microstructure at  $\text{Si}(100)$  surfaces. Our photoemission data are consistent with other photoemission data for low coverage Ni on  $\text{Si}(111)$  sur-

TABLE I. Diffused Ni super lattice models and parameters. Model I, all interstitial voids in the Si host lattice occupied (Ref. 6); model II, every second tetrahedral interstitial void occupied in Si lattice (this work); silicon rich ordered silicide  $\text{NiSi}_2$ .

	Diffusion-layer structure		Silicide $\text{NiSi}_2$
	Model I	Model II	
Ni-atom sublattice	Diamond	fcc	fcc
Lattice constant	$5.42 \text{ \AA}$	$5.42 \text{ \AA}$	$5.41 \text{ \AA}$
Ni atomic density	$0.05 \text{ atoms/\AA}^3$	$0.025 \text{ atoms/\AA}^3$	$0.0253 \text{ atoms/\AA}^3$
Ni-Ni neighbor distances (coordination)	$2.35 \text{ \AA}$ (4) $3.84 \text{ \AA}$ (8) $4.50 \text{ \AA}$ (8)	$3.84 \text{ \AA}$ (12) $5.42 \text{ \AA}$ (6)	$3.82 \text{ \AA}$ (12) $5.41 \text{ \AA}$ (6)

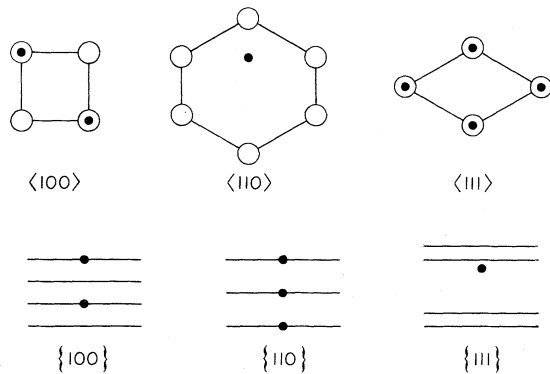


FIG. 3. Projected positions of the tetrahedral sites (full circles), occupied by the Ni atoms, along the various major channeling directions of the diamond lattice. The Si atomic rows are represented by open circles and the Si atomic planes are represented by solid lines.

faces,<sup>8</sup> and our new model is not necessarily in conflict with the channeling data. Both models are based on Ni atoms occupying tetrahedral sites, and both models will yield similar ion channeling angular patterns provided the diffused Ni atoms do not occupy tetrahedral sites which form a single macroscopic domain. If this occurs (which is likely in annealed samples) one would again expect symmetric scattering in ion scattering angular scans obtained by tilting the crystal around  $\langle 100 \rangle$  and  $\langle 111 \rangle$  directions and  $\{100\}$  and  $\{110\}$  planes but asymmetric scattering around  $\langle 110 \rangle$  directions and  $\{111\}$  planes. It is interesting to note that the data reported by Cheung and Mayer<sup>6</sup> do suggest some asymmetry in these cases.

We are pleased to acknowledge useful discussions with L. Kleinman and D. M. Bylander. This work was supported by the Joint Services Electronics Program under Grant No. F49620-77-C-0101 and by NSF under Grant No. DMR79-23629.

<sup>1</sup>J. Bardeen, Phys. Rev. **71**, 717 (1947).

<sup>2</sup>V. Heine, Phys. Rev. **138**, A1189 (1965).

<sup>3</sup>J. M. Andrews and J. C. Phillips, Phys. Rev. Lett. **35**, 56 (1975).

<sup>4</sup>J. L. Freeouf, Solid State Commun. **33**, 1059 (1980).

<sup>5</sup>N. W. Cheung, R. J. Culberston, L. C. Feldman, P. J. Silverman, K. W. West, and J. W. Mayer, Phys. Rev. Lett. **45**, 120 (1980).

<sup>6</sup>N. W. Cheung and J. W. Mayer, Phys. Rev. Lett. **46**, 671 (1981).

<sup>7</sup>P. J. Grunthaner, F. J. Grunthaner, and J. W. Mayer, J. Vac. Sci. Technol. **17**, 924 (1980).

<sup>8</sup>G. V. Hansson, R. F. Bachrach, R. S. Bauer, and P. Chiaradia, Phys. Rev. Lett. **46**, 1033 (1981).

<sup>9</sup>K. N. Tu, Appl. Phys. Lett. **27**, 221 (1975).

<sup>10</sup>J. L. Erskine, Phys. Rev. Lett. **45**, 1446 (1980).

<sup>11</sup>D. E. Eastman, J. Vac. Sci. Technol. **17**, 492 (1980).

<sup>12</sup>R. I. G. Uhrberg, G. V. Hansson, J. M. Nicholls, and S. A. Flodström, Phys. Rev. B **24**, 4684 (1981).

<sup>13</sup>Yu-Jeng Chang and J. L. Erskine (unpublished).

<sup>14</sup>D. M. Bylander, L. Kleinman, K. Mednick, and W. R. Grise, Phys. Rev. B (in press).

<sup>15</sup>Formation temperatures are Ni<sub>2</sub>Si, 200°C; NiSi, 400°C; NiSi<sub>2</sub>, 800°C. Yu-Jeng Chang and J. L. Erskine (unpublished).

<sup>16</sup>A. Franciosi, J. H. Weaver, and F. A. Schmidt, Phys. Rev. B **26**, 546 (1982).

<sup>17</sup>O. Bisi and C. Calandra, J. Phys. C **14**, 5479 (1981).